

- Suppl. 21, 433 (1966).
- ³D. H. Dickey and D. M. Larsen, Phys. Rev. Letters 20, 65 (1968).
- ⁴R. Kaplan and R. F. Wallis, Phys. Rev. Letters 20, 1499 (1968).
- ⁵D. H. Dickey, E. J. Johnson, and D. M. Larsen, Phys. Rev. Letters 18, 599 (1967).
- ⁶C. J. Summers, P. G. Harper, and S. D. Smith, Solid State Commun. 5, 615 (1967).
- ⁷C. J. Summers, R. B. Dennis, B. S. Wherrett, P. G. Harper, and S. D. Smith, Phys. Rev. 170, 755 (1968).
- ⁸J. Waldman, D. M. Larsen, P. E. Tannenwald, C. C. Bradley, D. R. Cohn, and B. Lax, Phys. Rev. Letters 23, 1033 (1969).
- ⁹B. D. McCombe and R. Kaplan, Phys. Rev. Letters 21, 756 (1968).
- ¹⁰*Light Scattering Spectra of Solids*, edited by G. B. Wright, (Springer-Verlag, New York, 1969).
- ¹¹P. A. Wolff, Phys. Rev. Letters 16, 225 (1966).
- ¹²P. M. Platzman, P. A. Wolff, and N. Tzoar, Phys. Rev. 174, 489 (1968).
- ¹³D. C. Hamilton and A. L. McWhorter, Phys. Rev. Letters 21, 309 (1968).
- ¹⁴P. A. Wolff, Phys. Rev. 171, 436 (1968).
- ¹⁵A. L. McWhorter and P. N. Argyres, Phys. Rev. Letters 21, 325 (1968).
- ¹⁶P. M. Platzman and N. Tzoar, Phys. Rev. 182, 510 (1969).
- ¹⁷F. A. Blum, Phys. Rev. B 1, 1125 (1970).
- ¹⁸H. Frohlich, *Polarons and Excitons*, edited by C. G. Kuper and G. D. Whitfield (Oliver and Boyd, Edinburgh, 1963), p. 1.
- ¹⁹P. G. Harper, Phys. Rev. 178, 1229 (1969).
- ²⁰A. A. Abrikosov, P. P. Gor'kov, and I. E. Dzyaloshinski, *Methods of Quantum Field Theory in Statistical Physics* (Prentice-Hall, Englewood Cliffs, N. J., 1963).
- ²¹T. M. Rice, Ann. Phys. (N. Y.) 31, 100 (1965).
- ²²H. Scher and T. Holstein, Phys. Rev. 148, 598 (1966).
- ²³J. M. Luttinger and J. C. Ward, Phys. Rev. 118, 1417 (1960).
- ²⁴L. I. Korovin and S. T. Pavlov, Zh. Eksperim. i Teor. Fiz. 53, 1708 (1967) [Soviet Phys. JETP 26, 979 (1968)].
- ²⁵M. Nakayama, J. Phys. Soc. Japan 27, 636 (1969).
- ²⁶T. Holstein, Ann. Phys. (N. Y.) 29, 410 (1964).
- ²⁷P. Nozières and D. Pines, Phys. Rev. 113, 1254 (1959).
- ²⁸N. D. Mermin and E. Canel, Ann. Phys. (Paris) 25, 247 (1964).
- ²⁹S. Iwasa, Y. Sawada, E. Burstein, and E. D. Palik, J. Phys. Soc. Japan Suppl. 21, 742 (1966).
- ³⁰R. Kaplan, E. D. Palik, R. F. Wallis, S. Iwasa, E. Burstein, and Y. Sawada, Phys. Rev. Letters 18, 159 (1967).
- ³¹E. J. Johnson and K. L. Ngai (unpublished).
- ³²R. Bowers and Y. Yafet, Phys. Rev. 115, 1165 (1959).
- ³³B. Lax, J. G. Mavroides, H. J. Zeiger, and R. J. Keyes, Phys. Rev. 122, 31 (1961).
- ³⁴E. J. Johnson and D. H. Dickey, Phys. Rev. B 1, 2676 (1970).
- ³⁵E. J. Johnson and D. H. Dickey, in Proceedings of the Electronic Density of States Conference, Natl. Bur. Std. (U. S.), 1970 (unpublished).

Piezorefectivity of Gallium Arsenide[†]

J. E. Wells and P. Handler

Department of Physics and Materials Research Laboratory, University of Illinois, Urbana, Illinois 61801

(Received 24 February 1970)

The response of the reflectivity spectrum of single-crystal gallium arsenide to uniaxial stress in the [001] and [111] directions was determined. Interband transitions were detected at 1.425 ± 0.015 , 1.76 ± 0.02 , 2.89 , 3.12 , and 4.5 eV. The direct edge at Γ is found to have a deformation potential ratio $d/b \approx 3.2$, using a stress-optical response model based on the Pikus-Bir Hamiltonian. The 2.89- and 3.12-eV spin-orbit-split transitions exhibit modulated reflectivity line shapes expected of Λ symmetry. Comparison is made with the stress-modulated response of a symmetry-related transition in germanium. The deformation-potential ratios $D_2^3/D_1^3 = -0.55 \pm 0.03$, $D_2^3/D_3^3 = 0.77 \pm 0.03$ have been derived. Comparison of the hydrostatic component of the perturbation with the energy derivative of the unmodulated reflectivity spectrum shows good agreement with a rigid-shift model. Finally, the 4.5-eV transition has shown a response to the stress perturbation indicative of a Δ symmetry.

I. INTRODUCTION

The band structure of gallium arsenide has been investigated in recent years by a number of differential optical-reflection techniques. Perturbations as electric fields,^{1,2} temperature,³ stress,⁴ or combinations of these effects⁵ have been used to

lift degeneracies and shift the energy bands in an attempt to obtain modulated reflectivity line shapes characteristic of the band symmetry.

Stress, as a perturbation, is, in many respects, the ideal approach to band-structure analysis. The band symmetries are easily traced from the undeformed to the deformed structure by elementary

group-theoretical techniques. In addition, matrix element selection rules can be determined through group-theoretical concepts. Such stress-optical techniques provide, in addition to transition energies and symmetries, the associated deformation potentials, describing band shifts and splittings under the applied perturbation. The dc stress technique found an early application in the measurements of Philipp *et al.*⁶ on germanium and silicon. However, the advantages of differential perturbation combined with the use of lock-in detection became clear with the electroreflectance work of Seraphin.⁷ Since that time, differential stress experiments have been conducted by a number of investigators, most recently by Sell and Kane,⁸ whose germanium results were interpreted in the light of a new symmetry formulation developed by Kane,⁹ including the Coulomb interaction in a symmetry analysis developed specifically for the diamond structure. Connection was made with the earlier work of Polak and Cardona⁵ who used the single-electron Pikus-Bir¹⁰ Hamiltonian to analyze germanium at the direct edge and at 2 eV, and applied the results toward the interpretation of a piezoelectroreflectance experiment.

In the work reported here, uniaxial stress has been employed in the [001] and [111] directions on T_d symmetry gallium arsenide, and differential reflectivity measurements made in the 1.1–4.6-eV region with the use of linearly polarized light. The spectra obtained at the fundamental edge (1.4 eV) have been interpreted in the framework of a deformation-potential model based on the Pikus-Bir Hamiltonian, considering matrix element variation and energy-band shifts under the applied perturbation.

Inasmuch as T_d symmetry is equivalent to diamond (O_h) symmetry minus the inversion operation, gallium arsenide and germanium have almost identical band symmetry in the Λ direction. Accordingly, line shapes deduced at 2 eV by Sell and Kane⁸ for germanium and interpreted as Λ symmetry might be expected to exhibit a marked similarity to the 3-eV gallium arsenide spectra, interpreted in earlier work⁵ as lying along the Λ symmetry line. Such similarity has been observed.

Finally, a line shape interpreted as a Δ symmetry has been observed at the upper end of the system range, a limit imposed by low-energy scatter light, predominant above 4.6 eV.

II. EXPERIMENT

Single-crystal gallium arsenide, dopant level $6.5 \times 10^{14} \text{ cm}^{-3}$, was obtained from the Monsanto Corporation.¹¹ The [001] and [111] directions were located in (110)-face wafers to within 1° , using Laue x-ray patterns. Surface preparation consisted

of 6- and 1- μ diamond polish on a rotary lap, followed by 0.05% bromine in methanol etch, also on a rotary lap. Finally, the sample was ground to 5 mil and bonded to a Clevite¹² bender bimorph with epoxy. The transducer was itself bonded to a brass-wedge support, enhancing a longitudinal resonance at 1 kHz.

A 1000-W Sylvania sun gun served as light source below 1.8 eV. Above 1.8 eV, a 75-W PEK xenon arc was employed. A Perkin-Elmer 210-B monochromator fitted with 1200-, 1800-, and 3600-line/mm gratings covered the full energy range under consideration. At low energies, polarizers were Polaroid HR polyvinyl film. The visible and ultraviolet polarizer was Polaroid HNP'B. Low-energy detection was provided by an EMI 9684B S-1 response phototube. Above 1.8 eV, an EMI 9558 S-20 response tube was employed. The optical beam was focused to dimensions $1 \times 3 \text{ mm}$ at near-normal incidence on the sample and refocused on the detector cathode, thus minimizing the usual "error signal" inherent in piezo-optical work.⁴

A PAR HR-8 lock-in amplifier used in the internal mode provided, with amplification, the driving voltage for the stress transducer, operated at resonance near 1 kHz. The high electromechanical response made 15-V rms an adequate driving level. A servomotor used in a feedback loop with a programmable power supply kept the dc photovoltage a constant 6 V, making the stress modulation signal, extracted by the HR-8, directly proportional to the differential reflectivity spectrum $\Delta R/R$.

III. THEORY OF STRESS-OPTICAL RESPONSE

The differential reflectivity tensor $\Delta R/R$ can be related to the stress (σ) and compliance tensors (S) by a fourth-rank tensor $Q^{8,13}$:

$$\Delta R/R_{ij} = Q_{ijkl} S_{klmn} \sigma_{mn}. \quad (1)$$

With uniaxial stress along the $\vec{\sigma}$ direction and light polarization $\vec{\eta}$, the effective value of $\Delta R/R$ is

$$\frac{\Delta R}{R} \Big|_{\vec{\sigma}} = \frac{\Delta R}{R} \Big|_{ij} \eta_i \eta_j. \quad (2)$$

Similarly, the stress-induced variation in the dielectric constant tensor has imaginary component

$$\Delta \epsilon_{ij} = W_{ijkl} S_{klmn} \sigma_{mn}, \quad (3)$$

$$\Delta \epsilon \Big|_{\vec{\eta}} = \Delta \epsilon_{ij} \eta_i \eta_j. \quad (4)$$

Both Q and W have only three nonzero terms for cubic crystals, denoted in the usual reduced notation¹⁴ as Q_{11} , Q_{12} , Q_{44} and W_{11} , W_{12} , W_{44} . Since three stress-polarization measurements are suf-

ficient to specify these stress-optical tensors, a fourth stress polarization should exhibit a linear dependence on the other three. In our notation,

$$\Delta\epsilon \left| \begin{smallmatrix} 11\bar{2} \\ 111 \end{smallmatrix} \right\rangle = \Delta\epsilon \left| \begin{smallmatrix} 110 \\ 001 \end{smallmatrix} \right\rangle + \frac{1}{2} (\Delta\epsilon \left| \begin{smallmatrix} 001 \\ 001 \end{smallmatrix} \right\rangle - \Delta\epsilon \left| \begin{smallmatrix} 111 \\ 111 \end{smallmatrix} \right\rangle). \quad (5)$$

An analogous relation holds for the four differential reflectivity measurements. $\Delta\epsilon$ is derivable from the differential reflectivity spectrum in the usual fashion.⁸

At the fundamental edge Pollak and Cardona have calculated, using the Pikus-Bir Hamiltonian, matrix element alterations and transition energy shifts as a result of uniaxial stress. Matrix element alteration contributes terms to $\Delta\epsilon$ proportional to ϵ , negligible in the vicinity of a semiconductor fundamental edge. Energy shifts, however, give terms varying as $d\epsilon/dE$. It is calculated that

$$\Delta\epsilon \left| \begin{smallmatrix} 001 \\ 001 \end{smallmatrix} \right\rangle \simeq -\frac{d\epsilon}{dE} (\delta E_H - \frac{1}{2} \delta E_{001}), \quad (6)$$

$$\Delta\epsilon \left| \begin{smallmatrix} 110 \\ 001 \end{smallmatrix} \right\rangle \simeq -\frac{d\epsilon}{dE} (\delta E_H + \frac{1}{4} \delta E_{001}),$$

where

$$\delta E_H = a (S_{11} + 2 S_{12}) \sigma, \quad (7)$$

$$\delta E_{001} = 2b (S_{11} - S_{12}) \sigma.$$

a and b are the Pikus-Bir deformation potentials relevant to hydrostatic and (001) uniaxial stress, respectively, while σ is the applied stress magnitude. The same expressions are valid for (111) stress with the replacement

$$\delta E_{001} \rightarrow \delta E_{111} = (d/\sqrt{3}) S_{44} \sigma, \quad (8)$$

introducing the deformation potential d , relevant to (111) stress.

At 3 eV, it becomes convenient to discuss results in terms of linear combinations of the fundamental data, and we define the following symmetry-related functions^{8, 13}:

$$W_H = (W_{11} + 2W_{12}) \sigma,$$

$$W_\Delta = (W_{11} - W_{12}) \sigma, \quad (9)$$

$$W_\Lambda = W_{44} \sigma.$$

Q_H , Q_Δ , and Q_Λ have analogous definitions. Taking the matrix element alterations and energy shifts provided by Pollak and Cardona, who assume the 3-eV gallium arsenide structure is of Λ symmetry,¹⁵

$$W_H = -3\mathcal{E}_1 \sigma \frac{d\epsilon}{dE},$$

$$W_\Delta = (3b/\Delta_1) \sigma (\epsilon^+ - \epsilon^-), \quad (10)$$

$$W_\Lambda = \frac{1}{3} \mathcal{E}_2 \sigma \frac{d\epsilon}{dE} - \frac{4d\sigma}{\sqrt{3}\Delta_1} (\epsilon^+ - \epsilon^-).$$

Accordingly,

$$W_\Lambda = -\frac{1}{9} (\mathcal{E}_2/\mathcal{E}_1) W_H + (4d/3\sqrt{3}b) W_\Delta. \quad (11)$$

Here \mathcal{E}_1 and \mathcal{E}_2 are the Brooks-notation deformation potentials,⁵ and Δ_1 is the magnitude of the spin-orbit energy splitting. ϵ^- and ϵ^+ are the portions of the dielectric constant associated, respectively, with transitions from the $\Lambda_4 + \Lambda_5$ and Λ_6 spin-orbit-split valence bands: $\epsilon = \epsilon^+ + \epsilon^-$. Note that there are only two independent stress-optical constants, exhibiting functional dependence on $(\epsilon^+ - \epsilon^-)$ and $d\epsilon/dE$.

Sell and Kane have shown that such a functional dependence should also hold in the Coulombic model. Assuming $\Lambda(L)$ symmetry transitions arising in the O_h structure between bands of symmetries,

$$\Lambda_4 + \Lambda_5 \rightarrow \Lambda_6, \quad \Lambda_6 \rightarrow \Lambda_6,$$

they show

$$W_\Lambda = -\frac{1}{6} (D_1^5/D_1^1) W_H + \frac{2}{3} (D_3^5/D_3^3) W_\Delta. \quad (12)$$

An approximate linear relationship with the same coefficients is also shown to hold for Q_Λ as a function of Q_H and Q_Δ . The above equations serve to introduce the Sell-Kane deformation-potential ratios D_1^5/D_1^1 and D_3^5/D_3^3 . Inasmuch as the germanium and gallium arsenide band symmetries are the same in the Λ direction, the same results apply for gallium arsenide and provide the correlation between the Coulombic model of Sell and Kane and the single-electron Hamiltonian utilized by Pollak and Cardona.

The 4.5-eV structure, thought to be of Δ symmetry,² has not been analyzed by Pollak and Cardona. Reference is made to the Coulombic model of Sell and Kane. The relative weakness of the structure precludes the possibility of deformation-potential assessment.

IV. RESULTS

The differential reflectivity spectra for the four stress-polarization geometries considered are presented in Fig. 1. The data have been adjusted to a zero below 1.1 eV. As a check on the internal consistency of the measurements, a least-square fit of the form

$$\frac{\Delta R}{R} \left| \begin{smallmatrix} 11\bar{2} \\ 111 \end{smallmatrix} \right\rangle = A \frac{\Delta R}{R} \left| \begin{smallmatrix} 001 \\ 001 \end{smallmatrix} \right\rangle + B \frac{\Delta R}{R} \left| \begin{smallmatrix} 110 \\ 001 \end{smallmatrix} \right\rangle + C \frac{\Delta R}{R} \left| \begin{smallmatrix} 111 \\ 111 \end{smallmatrix} \right\rangle + D \quad (13)$$

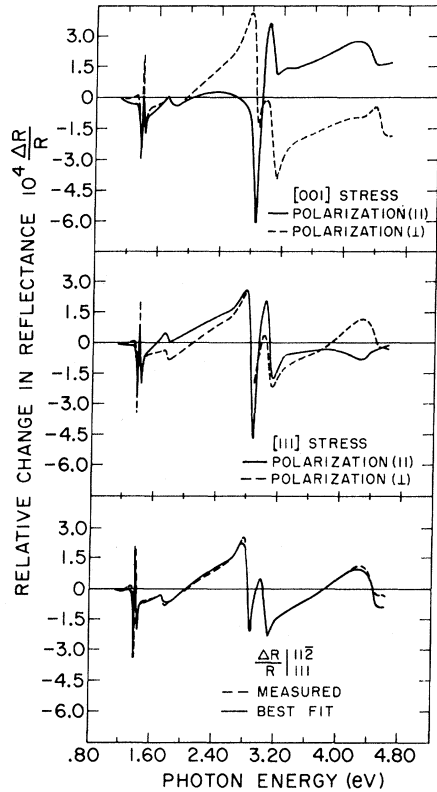


FIG. 1. Differential reflectivity spectra.

has been performed, giving each point in the interval to 4.1 eV weight 1, above 4.1 eV weight 0.

The least-square best fit is presented in Fig. 1, the coefficients of the fit being tabulated in Table I.

The parameter D has been introduced to account for the possibility of a wavelength-insensitive error in the differential measurements. The low value (1% of scale) of the parameter D shows that proper compensation for any offset signal has been made in the original measurements.

A. Fundamental Edge: E_0

The fundamental edge data, analyzed for $\Delta\epsilon$, are presented in Fig. 2. A point of note is the same wavelength dependence for all four scans, a response predicted by the model presented in Eqs. (6),

TABLE I. Least-squares fit for $[\Delta R/R]_{111}^{112}$

	Theory	Best fit	Error (%)
A	0.5	0.53	6
B	1.0	0.98	2
C	-0.5	-0.54	8
D	0	-0.33×10^{-5}	...

which show a wavelength dependence for $\Delta\epsilon$ at E_0 dependent on $d\epsilon/dE$ alone. The particular stress-polarization geometry merely lends a scaling factor to the $d\epsilon/dE$ wavelength dependence. Also of note is the approximate equivalence of line shape and amplitude of $\Delta\epsilon \left| \begin{smallmatrix} 001 \\ 001 \end{smallmatrix} \right|$ versus $\Delta\epsilon \left| \begin{smallmatrix} 111 \\ 111 \end{smallmatrix} \right|$ and $\Delta\epsilon \left| \begin{smallmatrix} 110 \\ 001 \end{smallmatrix} \right|$ versus $\Delta\epsilon \left| \begin{smallmatrix} 112 \\ 111 \end{smallmatrix} \right|$. Such would occur if $\delta E_{001} = \delta E_{111}$, implying $d \approx 3.2b$. That the equality is not exact is demonstrated by the (110) piezoelectroreflectance measurements of Pollak and Cardona,⁵ who show directly the existence of two stress-split structures, possible only if $\delta E_{001} \neq \delta E_{111}$. However, it should be noted that the model presented here predicts, on the basis of previous assessments⁵ of the deformation potentials (a, b, d), a somewhat larger value for $\Delta\epsilon \left| \begin{smallmatrix} 110 \\ 001 \end{smallmatrix} \right| / \Delta\epsilon \left| \begin{smallmatrix} 001 \\ 001 \end{smallmatrix} \right|$ and $\Delta\epsilon \left| \begin{smallmatrix} 112 \\ 111 \end{smallmatrix} \right| / \Delta\epsilon \left| \begin{smallmatrix} 111 \\ 111 \end{smallmatrix} \right|$ than actually occurs in these results and in the earlier work of Balslev⁴ at 100 °K.

The transition usually associated with the spin-orbit-split valence band at Γ , $E_0 + \Delta_0$ has been detected at 1.76 eV and appears in the differential reflectivity spectra of Fig. 1. The calculated $\Delta\epsilon$ is displayed in Fig. 2.

B. 3-eV Structure: $E_1, E_1 + \Delta_1$

The 3-eV differential reflectivity scans are presented in Fig. 1. The anisotropy of the 3-eV measurements is in marked contrast to the fundamental edge results, indicating a transition in \bar{K} space away from Γ .

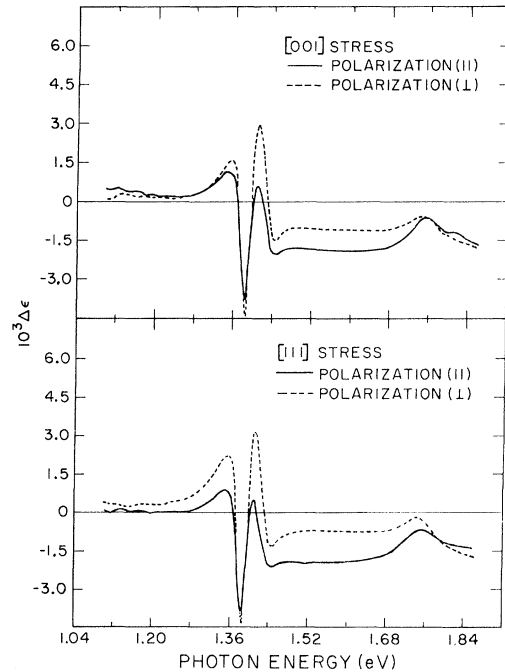


FIG. 2. Stress-induced alteration in the imaginary component of the dielectric constant.

It should also be noted that one of the four differential scans differs from the others in the sense that it exhibits a peak-antipeak behavior. The other three stress-polarization geometries exhibit a sequence of four peaks. The unique measurement is $(\Delta R/R)|_{001}^{001}$. It is only for this stress-polarization geometry that the eight proposed Λ ellipsoids would remain equivalent in the stress-deformed crystal. The other three stress-polarization geometries distinguish between the Λ ellipsoids, indicating this transition is of Λ symmetry.

The symmetry-related linear combinations of the fundamental data have been presented in Fig. 3. Reference to the germanium results of Sell and Kane⁸ indicates a marked similarity of line shapes between the 2-eV germanium scans [assigned Λ (L) symmetry] and the 3-eV gallium arsenide results, a further indication of the probable origin of the transition along the Λ direction.

According to theory,⁸ Q_H is related to the derivative of the unstrained reflectivity curves by the equation

$$Q_H = -3\epsilon_1\sigma \frac{d \ln R}{dE}. \quad (14)$$

The fine-structure reflectivity data of Lukes and Schmidt¹⁵ have been used to perform the derivative calculation, using a five-point derivative routine. The scaling factor $-3\epsilon_1\sigma$ was found to be 3.75×10^9 eV dyn/cm². However, to provide the correlation shown in Fig. 3, the Lukes-Schmidt data had

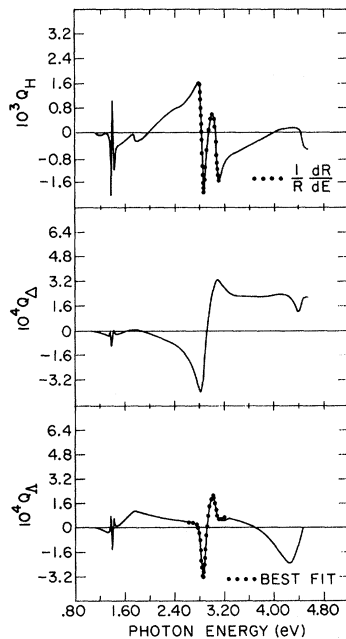


FIG. 3. Symmetry-related differential reflectivity spectra (units of 10^{12} dyn/cm²).

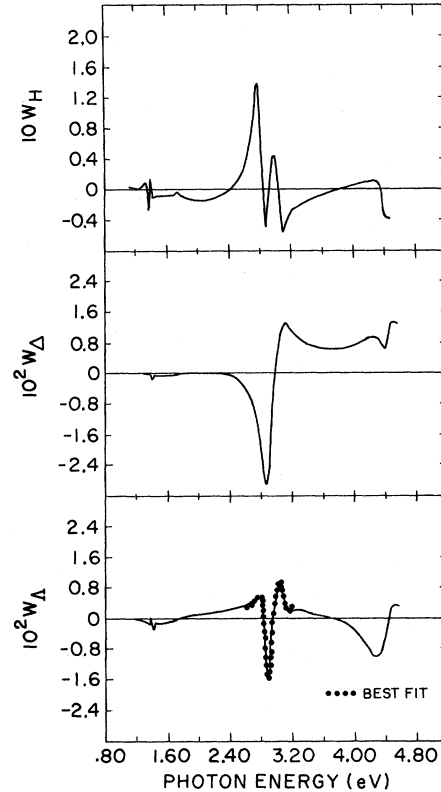


FIG. 4. Symmetry-related differential dielectric constant spectra (units of 10^{12} dyn/cm²).

to be shifted 60 meV toward lower energy. A similar shift of 30 meV was necessary to provide the correlation between the results of Sell and Kane⁸ and the fine-structure germanium reflectivity curves of Potter,¹⁶ pointing to the desirability of performing both differential and unperturbed reflectivity measurements on the same crystals.¹³

Since Q_H is a unitary symmetry deformation, Q_H line shapes should be similar to the perturbation produced by temperature modulation. Remarkable qualitative agreement exists between our work and the temperature modulation work of Matatagui *et al.*³ The principal variance is in the observed strength of the direct-edge transition in comparison to the 3-eV structure. The direct edge appears much stronger in our work.

The symmetry-related differential reflectivity spectra of Fig. 3 have been analyzed to obtain W_H , W_A , W_L , as presented in Fig. 4. Since W_H , accord-

TABLE II. Least-squares fit for Q_A and W_A .

	A	B	C
Q fit	0.09	0.50	1.4×10^{-5}
W fit	0.10	0.46	2.2×10^{-3}

ing to Eq. (10), is proportional to $d\epsilon/dE$, the large negative peaks appearing in this spectrum have been considered representative of the transition energies. The peaks appear at 2.89 and 3.12 eV, giving a spin-orbit splitting of 0.33 eV.

As noted in Eq. (11), W_A should be representable as a linear combination of W_H and W_Δ , the coefficients of the fit being related to the deformation potentials. Further, as mentioned, the same relationship should hold approximately for Q_A as a function of Q_H and Q_Δ .

Accordingly, between 2.6 and 3.2 eV, least-squares fits have been made of the form

$$\begin{aligned} W_A &= A W_H + B W_\Delta + C, \\ Q_A &= A Q_H + B Q_\Delta + C. \end{aligned} \quad (15)$$

For the data presented, the Q - and W -fit coefficients are tabulated in Table II. The parameter C has been introduced to account for the possibility of improper zero adjustment of the differential reflectivity data, as well as for the possibility of significant contribution to the differential spectra from regions in \vec{k} space not localized about the critical point.

The Q - and W -fit coefficients are in reasonable agreement. The low value of C (1% of scale for the Q fit, 3% for the W fit) indicates little offset due to background or improper zero adjustment.

The deformation potentials have been calculated from the Q fit for three reasons. First, the Q -fit coefficients (except for C) do not depend on the adjustment of the zero level of the data. Second, no external information as optical constants (n, k) need be introduced. Third, the Q fit is localized in the 2.6–3.2-eV region whereas the W fit is sensitive to extrapolations of the primary data outside this region, as well as being subject to line-shape distortion as a result of improper zero adjustment of the differential reflectivity spectra. The deformation-potential ratios determined from the Q fit are

$$D_1^5/D_1^1 = -0.55 \pm 0.03, \quad D_3^5/D_3^3 = +0.77 \pm 0.03.$$

These values, as compared with the data of Pollak and Cardona through Eqs. (10) and (11), are

$$D_1^5/D_1^1 = -1.23_{-0.22}^{+0.26}, \quad D_3^5/D_3^3 = 3.46_{-0.52}^{+0.60}.$$

As noted, our value for D_1^5/D_1^1 is only $\frac{1}{2}$ that found by Pollak and Cardona,⁵ while D_3^5/D_3^3 varies by a factor 4. In comparing their germanium data with those of Pollak and Cardona, Sell and Kane get good agreement for the ratio D_1^5/D_1^1 , but note a factor of 4 variance in the ratio D_3^5/D_3^3 . The error estimates on their values as well as our own seem to lie outside the range suggested in the paper of Pollak and Cardona.

C. 4.5-eV Structure: $E_0, E_0 + \Delta_0$

The highest energy transition observed was at 4.5 eV, and is traditionally assigned Δ symmetry.² The weakness of the structure, coupled with the difficulty of obtaining measurement at higher energies, precludes the possibility of definitive statements. However, it might be observed that a line-shape uniqueness argument applied to the $(\Delta R/R)|_{111}$ measurement, which alone presents a minimum response at 4.5 eV, seems to agree with Δ symmetry for this structure.

V. CONCLUSION

The location of the critical points E_0 and $E_0 + \Delta_0$ have been established as 1.425 ± 0.015 and 1.76 ± 0.02 eV, respectively. The behavior of $\Delta\epsilon$ near the E_0 structure approximately isotropic in response to the applied stress perturbation confirms a Γ symmetry. The deformation-potential ratio d/b has been shown to be approximately 3.2.

The response to polarization and stress near 3 eV has been shown to be consistent with a model proposed for Λ symmetry. Critical points have been taken as 2.89 and 3.12 eV. Variance with the earlier work of Pollak and Cardona in the deformation-potential ratios has been detected, the values obtained here being

$$D_1^5/D_1^1 = -0.55 \pm 0.03,$$

$$D_3^5/D_3^3 = 0.77 \pm 0.03.$$

Finally, stress-polarization response at 4.5 eV suggests a Δ symmetry, in accordance with previous assessment.

[†]Work supported in part by the Advanced Research Projects Agency under Contract No. SD-131, and in part by the U. S. Army Research Office-Durham.

¹B. O. Seraphin, J. Appl. Phys. **37**, 721 (1966).

²M. Cardona, K. L. Shaklee, and F. H. Pollak, Phys. Rev. **154**, 696 (1967).

³E. Matatagui, A. G. Thompson, and M. Cardona, Phys. Rev. **176**, 950 (1968).

⁴I. Balslev, Phys. Rev. **143**, 636 (1966); W. E. Engeler,

H. Fritzche, M. Garfinkel, and J. J. Tiemann, Phys. Rev. Letters **14**, 1069 (1965); G. W. Gobeli and E. O. Kane, *ibid.* **15**, 142 (1965).

⁵F. H. Pollak and M. Cardona, Phys. Rev. **172**, 816 (1968).

⁶H. R. Phillipp, W. C. Dash, and H. Ehrenreich, Phys. Rev. **127**, 762 (1962).

⁷B. O. Seraphin, Phys. Rev. **140**, A1716 (1965).

⁸D. Sell and E. O. Kane, Phys. Rev. **185**, 1103 (1969).

- ⁹E. O. Kane, Phys. Rev. 178, 1368 (1969).
¹⁰G. E. Pikus and G. L. Bir, Fiz. Tverd. Tela 1, 154 (1959)[Soviet Phys. Solid State 1, 136 (1959)].
¹¹Monsanto Corp., 800 N. Lindbergh Blvd., St. Louis, Mo.
¹²Clevite Corp., Piezoelectric Div., 232 Forbes Road, Bedford, Ohio.
¹³U. Gerhardt, Phys. Rev. 172, 651 (1968).
¹⁴J. F. Nye, *Physical Properties of Crystals* (Oxford U.P., Oxford, England, 1967).
¹⁵F. Lukes and E. Schmidt, in *Proceedings of International Conference on the Physics of Semiconductors, Exeter*, July 1962, edited by E. Strickland, (The Institute of Physics and The Physical Society, London, 1962), pp. 389-394.
¹⁶R. F. Potter, Phys. Rev. 150, 562 (1966).

PHYSICAL REVIEW B

VOLUME 3, NUMBER 4

15 FEBRUARY 1971

Vibrational Dispersion and Small-Polaron Motion: Enhanced Diffusion*

David Emin

Sandia Laboratories, Albuquerque, New Mexico 87115

(Received 21 September 1970)

The one-dimensional molecular-crystal model of Holstein is utilized in a preliminary investigation of the effects of the dispersion of the longitudinal optical frequencies on the hopping motion of small polarons. In particular, this work raises the question of whether the lattice relaxes sufficiently rapidly after a small-polaron hop so that a subsequent hop of the excess carrier may be considered independent of the initial hop. To this end, Holstein's perturbative approach is applied in calculating the probability of an initial small-polaron jump being followed by another small-polaron hop at a time t later. Furthermore, the small-polaron drift mobility is calculated assuming that the polaron's jump rate is only influenced by its immediately preceding hop. It is found that, for the circumstance in which the average time between jumps is small compared with the relaxation time of the lattice, the activation energy characterizing the small-polaron drift mobility is smaller than that found for completely independent jumps. In fact, for appropriate choices of the physical parameters, the drift mobility may display a very mild temperature dependence, decreasing with increasing temperature at sufficiently high temperatures.

I. INTRODUCTION

It has been recognized for a long time that the placing of a stationary excess carrier in a lattice would in general polarize the neighboring region about the carrier in such a way that a potential well is produced about the carrier which tends to trap it at its position in the lattice. In particular, if the potential well associated with the carrier-induced distortion is sufficiently deep that a bound state is formed, the carrier will be unable to move unless accompanied by its induced lattice deformation. The unit comprising the carrier and its associated lattice distortion is called a polaron. Furthermore, in the situation in which the carrier is localized about a given lattice site with a spatial extent of the order of a lattice spacing, the polaron is referred to as a *small polaron*.¹

At sufficiently low temperatures the motion of a small polaron was shown to be describable in terms of motion in a small-polaron band, the width of which is a decreasing function of increasing tem-

perature.² In addition, Holstein showed that above a temperature which is characterized by the energy uncertainty associated with the finite lifetime of a carrier in a band state being of the order of the width of the small-polaron band, it is no longer appropriate to view the motion of the small polaron in terms of the band picture. In this high-temperature regime, the small polaron is pictured as essentially localized, moving through the lattice via a succession of thermally activated hops. The remainder of this paper shall be concerned solely with small-polaron motion in this hopping regime.

A number of theoretical papers have been concerned with the hopping motion of small polarons. These calculations have been carried out within two complementary approximation schemes. In particular, in the perturbative approach developed by Holstein² it was assumed that the carrier responds sufficiently slowly to the vibrational motion of the lattice so that it is not generally able to "follow" the lattice motion. Within this approach (a) the drift mobility was found to be thermally ac-